CHAOTIC MIXING OF MAGNETIC BEADS IN MICRO CELL SEPARATOR

Hiroaki Suzuki, Nobuhide Kasagi
Department of Mechanical Engineering, The University of Tokyo
Hongo, Bunkyo-ku, Tokyo 113-8656, Japan
hsuzuki@thtlab.t.u-tokyo.ac.jp, kasagi@thtlab.t.u-tokyo.ac.jp

Chih-Ming Ho
Department of Mechanical and Aerospace Engineering
University of California, Los Angeles
420 Westwood Plaza, Los Angeles, CA 90095, USA
chihming@ucla.edu

ABSTRACT

In micro-scale biological assay systems, the mixing of bio-molecules becomes a critical issue because of their small diffusivity. Chaotic features in a novel micro-mixer designed for cell separation system based on magnetic beads (Suzuki and Ho, 2002) is investigated in detail by means of numerical simulation. The mechanism and the optimum condition to lead the motion of magnetic beads to chaos are clarified. It is found that the chaotic mixing would significantly facilitate the attachment of magnetic beads onto bio-molecules, which practically do not occur without an external perturbation. Active micro-mixers achieve rapid and efficient mixing even in the creeping flow regime, which is not accomplished with the passive micro-mixers.

INTRODUCTION

The study of fluid flow and its control in micro-scale devices has been an active area of research because of the growing demand for the on-chip bio-chemical analysis systems, which are often called μ-TAS (micro Total Analysis Systems) or Lab-on-a-Chip (Manz et al., 1990; Burns et al., 1998; Oki et al., 2001). Since most of chemical and biological reaction processes are performed in liquid and suspension, the development of μ-TAS is intrinsically related with the development of micro fluidic devices (Ho, 2001).

In such small systems, the flow is unavoidably laminar due to its low Reynolds number. Conventional mixing schemes utilizing turbulence or flow separation cannot be used when the Reynolds number is less than ten. Since molecular diffusion is the only way to mix, it takes considerable time and thus limits the performance of the device. Especially in biological processes, diffusion of bio-molecules such as cell, protein, enzyme, antibody, and nucleic acid becomes much less efficient than that of water-soluble entities, since the diffusion coefficient due to the Brownian motion is inversely proportional to the diameter of suspended molecule (Einstein, 1905; Suzuki and Ho, 2002). Therefore, an excellent convective mixing scheme is strongly desired to enhance their reactions and thus to achieve rapid and efficient operation. Moreover, the reaction sites of bio-molecules are not necessarily distributed uniformly, so that the continuous stirring is preferred to further increase the chance of their collision.

In recent literatures, a number of micro mixing devices have been reported. They are divided into two categories, i.e., passive and active mixers. Passive mixers are those that require no extra energy input except for the constant pressure difference to drive the flow. The principle "lamination" has been firstly experimented, in which the flow is split into subsequent flows to reduce the diffusion length scale (Branebjerg et al., 1996; Möbius et al., 1995). More recently, the concept of "chaotic advection" has been utilized, in which a simple flow configuration in an Eulerian frame produces highly complicated pattern in a Lagrangian frame. For instance, 3-D serpentine channel (Liu et al., 2000) and herringbone-ridged channel (Stroock et al., 2002) have been shown to produce chaotic mixing pattern. The passive mixers have advantages in several regards, e.g., they work for any kind of species to be mixed, and require no external perturbing mechanism. However, the flow channel has to be three dimensional to produce chaotic mixing, and even so, a relatively long mixing length (>1cm) and large Reynolds number (Re>20) are necessary. Active mixers are defined as those that exert external, mostly time-dependent, perturbation over the flow field. Chaotic advection has also been utilized for active mixers, recently, to realize more rapid and efficient mixing. Lee et al. (2001) used a periodic pressure perturbation through the perpendicular side channels to impose stretching and folding of the interface of two streams. Deval et al. (2002) employed the time-varying dielectrophoretic force to induce chaotic motion on polymer particles suspended in water.

We proposed, fabricated, and tested a magnetic force driven chaotic micro-mixer, in which magnetic beads are stirred by the local time-dependent magnetic field (Suzuki and Ho, 2002). In molecular biology studies, magnetic beads (polymer micro spheres containing iron oxide) coated with ligand or antibody is used for selective separation of bio-molecules from the mixture. The target bio-molecules are labeled by beads by the antigen-antibody reaction, and then removed from the mixture with a permanent magnet. When this cell separation protocol is miniaturized, mixing of magnetic beads and bio-molecules becomes critically important, due to their very small diffusivity. The magnetic mixer developed in this study is to enhance the probability of attachment of the beads onto the target bio-molecules in the micro-channel by means of chaotic advection.

In this paper, we examine the chaotic features of the magnetic micro-mixer and characterize its performance. Dynamics of magnetic beads is investigated in detail through numerical simulation. Finally, the comparison between passive and active

mixers is discussed.

BASIC DESIGN OF MAGNETIC MICRO-MIXER

The conceptual diagram of the magnetic micro-mixer is illustrated in Fig. 1(a). It consists of micro-conductors embedded in the silicon substrate and a micro-channel formed on its top. The embedded high aspect-ratio conductors, which are fabricated by deep RIE etching followed by copper electroplating, allow a relatively large current (up to 1A) to generate a magnetic field strong enough to move magnetic beads. Two streams, i.e., biological fluid and magnetic bead suspension, flow in from respective inlets and meet together before the mixing region. Then, they are mixed to facilitate the biomolecule-bead conjugate. For the details of fabrication process, readers should refer to Suzuki and Ho (2002).

A basic unit of magnetic filed source is very simple: when an electric current is applied to a pair of parallel conductors, a magnetic field is generated so that the magnetic beads are attracted toward them. To estimate the magnetic force on beads, the magnetic field around the two infinite-long parallel conductors is calculated by Biot-Savart law (Fig. 1b). In micro-systems, the scale of the section of conductors becomes comparable with that of the device. Thus, the section of conductor is divided into small segments, and the magnetic field is calculated by integrating the contribution of each segment. In the figure, x and z represent streamwise and wall-normal directions, respectively (x=0 at the center of two conductors), and two conductors, whose width and depth are both 40μm, span at -60μm<x<-20μm and 20μm<x<60μm (shown as two squares). When an electric current of 0.5A is applied, the maximum magnetic induction of 40 Gauss is achieved near the conductors. Given the magnetic field $\boldsymbol{H}$, the magnetic force on a bead is calculated by

$$\boldsymbol{F}_m = (1 - N_d)\mu_0 \mu_r V_p (\boldsymbol{H} \cdot \nabla \boldsymbol{H}) \qquad (1)$$

where N_d is the demagnetizing factor (0.33 for a sphere), μ_0 is the permeability in vacuum, μ_r is the relative permeability, and V_p is the volume of magnetic material. When $\boldsymbol{F}_m$ is exerted, a magnetic bead starts to move and settles at the terminal velocity:

$$\boldsymbol{u}_p = \boldsymbol{F}_m / 3\pi\mu d_p \qquad (2)$$

where μ is the viscosity of ambient fluid and d_p is the diameter of a bead. $\boldsymbol{F}_m$ and $\boldsymbol{u}_p$ are calculated with the properties of magnetic beads used in the experiment (Spherotech, CM-10) shown in Table 1. Magnetic properties are measured by VSM (Vibration Sample Magnetometer; Digital Measurement System, VSM880).

In Fig. 2, x components of $\boldsymbol{F}_m$ and $\boldsymbol{u}_p$ at different z are plotted. The positive value represents the direction toward the center of the two conductors (toward left). It is shown that magnetic beads are attracted to accumulate at the inside edges of the conductors, where the plot of the magnetic force crosses the horizontal axis (x~20μm). The maximum force and velocity are derived near the outside edge (x~60μm), and are 0.3pN and 25μm/s, respectively.

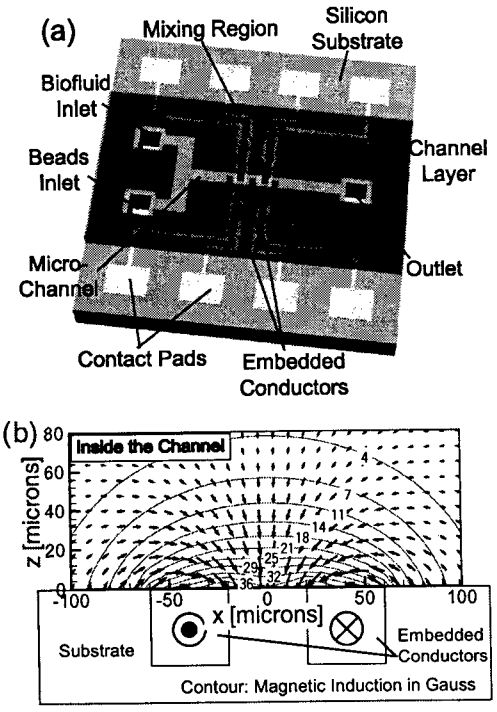

Fig. 1 (a) Conceptual diagram of the magnetic micro-mixer. (b) Cross-section of the mixing region along the channel showing magnetic field.

STRATEGY OF CHAOTIC MIXING

In the previous section, it is shown that magnetic beads can be manipulated with the local magnetic field generated by simple micro conductors. In this section, the strategy to realize an efficient mixing of beads is discussed.

In designing a mixing device, the concept of chaotic advection becomes a powerful tool, with which the complicated mixing pattern is realized even in creeping flows. It is recognized when the Lagrangian trajectory has a sensitive dependence on initial condition (Ottino, 1989). In such systems, the distance between initially nearby trajectories diverge exponentially fast, and the resultant state becomes unpredictable due to the ambient noise. It is known that even two-dimensional laminar flow can be chaotic when the time-dependency is added as another dimension. Stretching and folding of material element produce an exponential growth of the interface, leading to the chaotic state.

In open flow systems, chaotic advection can be realized by pushing and pulling the element between main flow and side channels/cavities (Lee et al., 2001; Deval et al., 2002). With

Table 1 Properties of magnetic beads (Spherotech, SPHERO™ CM-10).

Diameter	1.0-1.4 [μm]
Ion Oxide Content	~12 [wt%]
Average Density	1.58 [g/cm^3]
Saturation Magnetization	0.46 [Tesla]
Relative Permeability	11.3

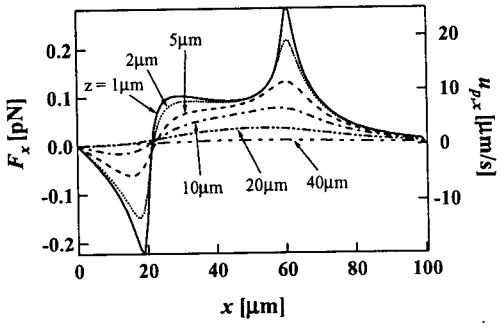

Fig. 2 Magnetic force and induced velocity on a bead with current of 0.5A.

magnetic force, however, only an attractive force can be achieved, so that magnetic beads pulled into the low velocity region (e.g. side cavity) will not come back to the high velocity region, and remain stuck there.

In Suzuki and Ho (2002), we demonstrated that the chaotic motion of magnetic beads can be achieved with a two dimensional serpentine channel and phase shift signal. Let us briefly introduce its design and mixing strategy here again. Figure 3 illustrates one unit of 2-D serpentine channel design, with four perpendicular electrodes shown as shaded lines. It repeats in x (streamwise) direction. The chaotic motion is induced on magnetic beads, flowing steadily otherwise, with time-dependent control signal (Phase Shift Signal) shown in Fig. 4. For instance, when electric current is applied to electrodes 3 and 4 at the phase (iv), magnetic beads flowing are attracted toward the low velocity region at the corner (arrow 1). At the other phase, e.g. phase (iii), current is applied to electrodes 2 and 3, and thus beads that had been drawn into the corner are pulled back to the mainstream (arrow 2). Attractive and repulsive motion can be mimicked by shifting the pair of working electrodes.

EXPERIMENT

Figure 5 shows a magnetic micro-mixer with a serpentine shaped channel fabricated according to the design presented in Fig. 3. Four mixing units are repeated in the mixing region. The unit length L, width W and height H of the channel are 320μm, 160μm and 35μm, respectively. Width and spacing of the conductors are both 40μm.

The mixing process of magnetic beads, when the phase shift signal is applied, is shown in Fig. 6. In Fig. 6(a), magnetic bead suspension is flowing in the lower side of the channel, while DI water is flowing in the upper side. The bulk flow rate is approximately 50nL/min, which corresponds to $Re = WV/\nu = 2.2\times10^{-2}$ (V: bulk mean velocity). The electric current applied is 0.7A. Without an external perturbation, beads do not spread across the streamline, and the interface of the bead suspension persists to the downstream. When the phase shift signal is applied, beads are stirred in a complicated manner, showing the stretching and folding pattern repeatedly (Fig. 6b). In the downstream, beads spread all over the channel and thus a well-mixed state is achieved (Fig. 6c).

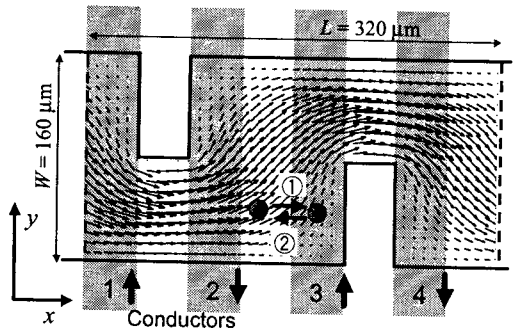

Fig. 3 Serpentine channel and perpendicular electrode configuration.

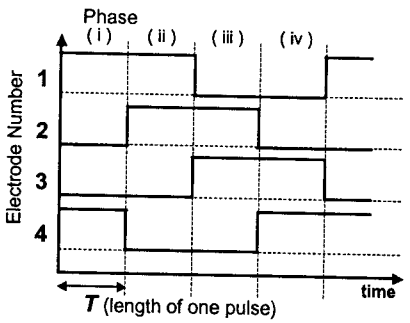

Fig. 4 Phase shift control signal.

NUMERICAL SIMULATION

In this section, two-dimensional numerical simulation is used to examine the motion of magnetic beads in the Lagrangian frame. In most of MEMS based fluidic devices, dimension in the out-of-plane direction (height) is much smaller than that in in-plane direction due to the intrinsic property of thin-film processes such as spin-coating, evaporation, and CVD. Thus, the physical phenomena in such devices are often comprehended by two-dimensional observation.

The Lagrangian tracking of magnetic beads has been conducted with one-way coupling scheme. Firstly, the steady 2-D velocity field is computed with a commercial CFD code based on the finite volume method (CFD-ACE+, CFD Research Corp.) on 80×40 grid points. The bulk mean velocity V is set to 80μm/s ($Re = 1.3\times10^{-2}$). Then, the trajectories of beads $\boldsymbol{x}_p$ are calculated by integrating the sum of the induced velocities due to the fluidic drag and magnetic force, i.e.,

$$\boldsymbol{x}_p(t) = \int \{\boldsymbol{v}_f(x) + \boldsymbol{u}_p(x,t)\}\, dt \qquad (3)$$

with 4th order Runge-Kutta method ($\boldsymbol{v}_f$: steady velocity field).

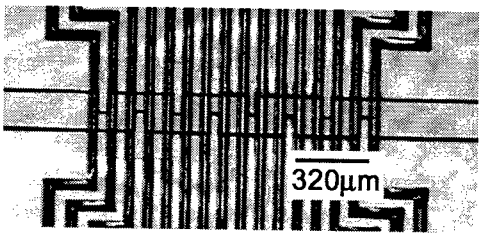

Fig. 5 Fabricated magnetic micro-mixer with a serpentine shaped channel.

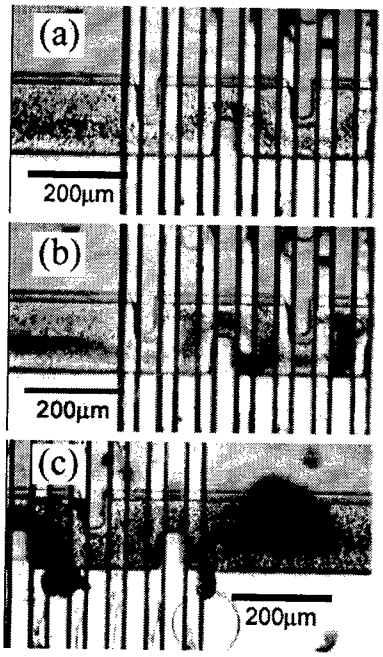

Fig. 6 (a) No magnetic force is applied. (b) Mixing pattern when phase shift signal is applied. (c) Magnetic beads spread all over the channel at the downstream.

The relaxation time τ_p of magnetic beads used in this study is 1.2×10^{-7} [s], which is much smaller than the time scale of the control signal (~1[s]). Hence, magnetic beads react to the magnetic force as well as the flow drag with no delay. The error due to neglecting acceleration relative to the magnitude of u_p is on the order of τ_p (Suzuki, 2003) and eq. (3) becomes valid. The number of the grids and time step is confirmed to be sufficient. Magnetic force at each phase is calculated from Biot-Savart's law and eq. (1). Motion of beads is examined by changing two parameters, the maximum value of bead velocity induced by magnetic force ($u_{p,max}/V$) and driving frequency ($St=W/VT$).

Flow Visualization

Figure 7 depicts the distribution of 7800 magnetic beads, initially distributed in the shaded area, after 12 seconds (the time the beads pass approximately 6 units). Without magnetic force, they exactly follow the streamline and the resultant pattern is regular (Fig. 7a). On the other hand, when the phase shift signal is applied (St=8.3, $u_{p,max}/V$=1.0), stretching and folding pattern is induced repeatedly and chaos-like pattern is obtained in the whole domain (Fig. 7b).

From close observation of the lump deformation, two mechanisms to create stretching and folding are found to exist, which are achieved by pushing and pulling the beads in and out of the low velocity region at the corner.

Figure 8 illustrates the successive images of beads to show the stretching and folding mechanism attained behind an obstacle. In Fig. 8(1)-(3), current is applied to the first two electrodes, so that beads are attracted toward them (small arrows in Fig. 8-1). While beads closer to the wall are pulled into the corner (arrow 1 in Fig. 8-2), those near the center remain being advected by the main flow (arrow 2). Hence, a small fold is induced on the lump of beads (Fig. 8-3). As the current turned off, beads are further advected downstream toward the next narrow section, where this fold is stretched by the shear (arrow 3 in Fig. 8-5). Eventually, a large folding pattern is created (Fig. 8-6).

On the other hand, Fig. 9 illustrates the mechanism attained in front of an obstacle. Fig. 9(1) depicts the instance right before the electrodes 2 and 3 are turned on. Note that a line of beads is aligned along the front side of the second obstacle. As the current is applied, it is pulled back to the left (Fig. 9-2). At this moment, they suffer upward velocity from the flow. When the current is turned off, a small folding pattern appears above the obstacle (Fig. 9-3).

Therefore, the stretching and folding mechanism that arises behind the obstacle is shown to play a primary role to the global mixing, while that in front of the obstacle contributes only to local and small folding patterns.

Quantitative Analysis

Divergence of the initial condition, which is one of the manifestations of chaos, is quantified by means of Lyapunov exponent (hereafter, LE). It represents an exponential rate of stretching and defined as:

$$\sigma = \lim_{t\to\infty}\left[\frac{1}{t}\ln\left(\frac{|dx(t)|}{|dx(0)|}\right)\right] \qquad (4)$$

where t is time, and $|dx(0)|$ and $|dx(t)|$ are distance between two points at time zero and t, respectively. If σ is positive non-zero value, then $|dx(t)| = |dx(0)|\exp(\sigma t)$ and the distance of two initially nearby points diverges exponentially with time. Originally, LE is defined as a spectrum, which has a dimension of phase space. However, it is suffice to measure its largest component (Largest LE) to characterize the system, which is much simpler in calculation. For implementation, the Wolf's method (Wolf et al., 1985) is employed, and an average of 88 initial points uniformly distributed in the channel is taken to extract the characteristics of the system.

Figure 10 shows some examples of the convergence of the largest LE calculation. The solid line represents the case of St=7.6 and $u_{p,max}/V$=1.5, where a good mixing pattern is observed such as the one shown in Fig. 8(b). In this case, the LE converges rapidly just after 50 seconds (that corresponds to the time a bead passes ~25 units), and stays constant (~0.38). The system is chaotic in such amplitude and frequency domain. When there is no disturbance (dashed line), the LE gradually approaches to zero, but it takes much longer time to converge. Broken line represents the case of St=13 and $u_{p,max}/V$=0.5, where mixing is very poor. Due to the high driving frequency and the weak magnetic force, initial condition drawn in Fig. 8 stay in the lower half of the channel, so that global mixing is not achieved in this domain. In such a case, the LE converges to a negative value, which indicates that the initial condition contracts.

Figure 11 shows the largest LE after 240 seconds with vary-

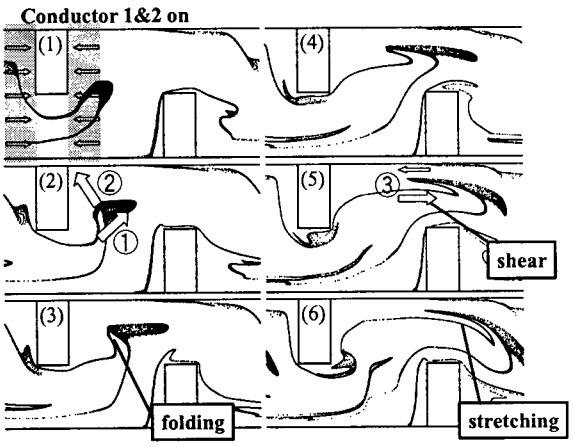

Fig. 8 Dominant mechanism to create stretching and folding behind the obstacle.

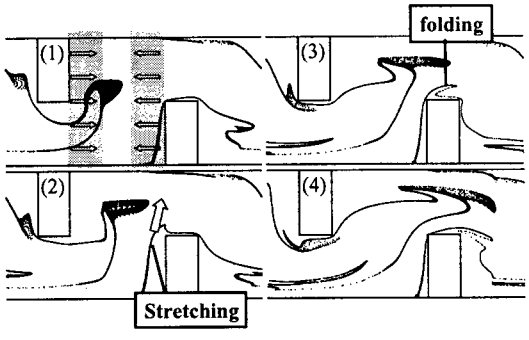

Fig. 9 Mechanism to create stretching and folding in front of the obstacle.

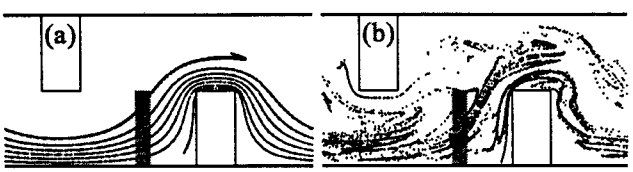

Fig. 7 Deformation of the lump of magnetic beads (a) without and (b) with phase shift signal (St=8.3, $u_{p,max}/V$=1.0).

ing driving frequency (St). The dotted horizontal line represents the value when no external disturbance is applied, and other lines show the LEs with the phase shift signal of different $u_{p,max}/V$. The exponent takes positive values at $5<St<10$, regardless of $u_{p,max}/V$. It indicates that the exponential divergence of initial condition is accomplished in this driving frequency regime. The optimum frequency lies around St_{opt}=7~8 to drive the flow toward chaos.

Figure 12 shows the deformation of the lump of beads when St is smaller and larger than St_{opt} with the same initial condition as Fig. 8. When $St<St_{opt}$, magnetic beads are attracted toward the electrodes for a longer time period, so that they tend to accumulate at the edge of the electrodes for a certain period. Thus, global mixing is not achieved since continuous stirring is prohibited (Fig. 12a). When $St>St_{opt}$, global mixing is not achieved either, since only local and small undulations are created with higher frequency. Therefore, it is concluded that the matching of the driving frequency and the flow time constant contributes to larger LE and thus an excellent mixing.

Beads and Cell Attachment

The goal of designing our magnetic mixer is to enhance the attachment of magnetic beads to bio-molecules, which are flowing in parallel. The attachment rate is calculated as follows. As an initial condition, 100 non-magnetic particles (diameter d_c=3.5μm which mimic cells) and 1340 magnetic beads (d_p=1μm) are distributed in the upper and lower side of the center streamline, respectively. As the phase shift signal is applied, only magnetic beads are stirred by time-dependent magnetic field, while non-magnetic particles flow unaffectedly. When the distance between a cell and a bead becomes less than the sum of their radii, the bead is considered to be attached to the cell, and then vanished.

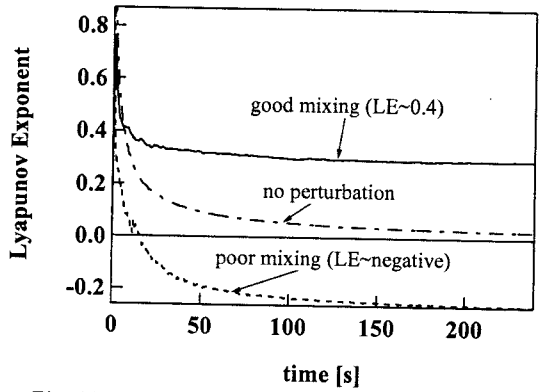

Fig. 10 Convergence of the largest Lyapunov exponent.

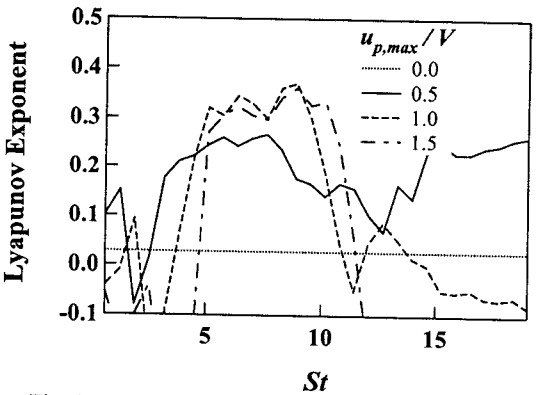

Fig. 11 Frequency dependence of the largest Lyapunov exponent.

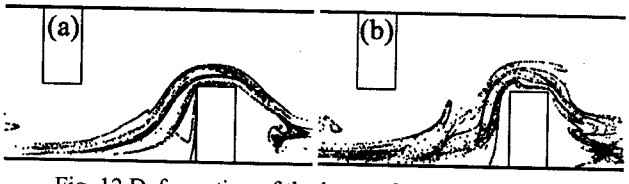

Fig. 12 Deformation of the lump of magnetic beads.
(a) St=4.5, $u_{p,max}/V$=1.0 (b) St=11.4, $u_{p,max}/V$=1.0.

Figure 13 shows the ratio of cells on which magnetic beads are attached after 12 seconds (~6 mixing unites), at various St and $u_{p,max}/V$. The shaded area shows the frequency and amplitude regime with which more than 50% of cells are labeled. It is clear that, regardless of $u_{p,max}/V$, the best yield is derived at St~8. This driving frequency corresponds to St_{opt} of the Lyapunov exponent. Thus, the probability of attachment of beads onto biomolecules should be greatly increased in the chaotic regime.

COMPARISON WITH A PASSIVE MIXER

In this section, the performance of the present mixer is compared with the 3-D serpentine passive mixer proposed in Beebe et al. (2001), which is schematically shown in Fig. 14. To understand the phenomena in this configuration, its steady flow field is computed on 80×40×40 grid points, and the trajectories of fluid particles are calculated by Runge-Kutta method. Velocity between the grids is obtained with 4th order Lagrange interpolation. Poincaré section, which is a plot of successive set of intersection of the trajectories, is created at x=0 (Fig. 15a-c). The similar pattern to Fig. 8 in Beebe et al. (2001) is successfully reproduced. The pattern of Poincaré section is regular at Re=1, showing that the flow is non-chaotic. When Re=10~20, the plot starts to show the random pattern at the periphery. However, the KAM (Kolmogorov-Arnold-Moser) surfaces, which are seen as circles near the center in Fig. 14b and c, still remain. The fluid particles flowing inside KAM tube will never be mixed with the rest (Ottino, 1990). The system becomes almost fully chaotic at Re=50. The reason to show the chaotic behavior at Re>20 is that chaotic flow in 3-D steady flow utilizes the flow separation, which gives rise to the large shear to create stretching, and the recirculation to create folding.

Although Poincaré section is an easy and convenient way to comprehend the characteristics of the system, it lacks information of time. In the mixing problem, reduction of operation time and device length are also the important aspects as well as the resulting state. Figure 16 shows the distribution of beads/tracers at different time period in (a) 2-D magnetic mixer, (b) 3-D pas-

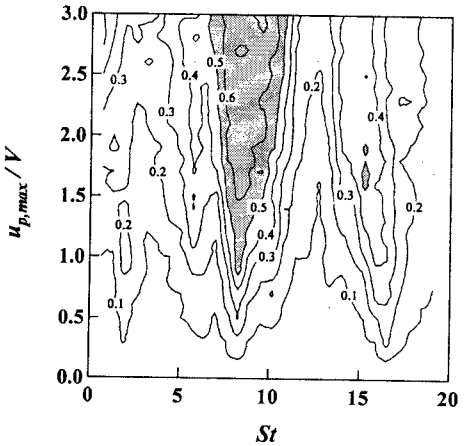

Fig. 13 Ratio of tagged cell after 12 seconds at various St and $u_{p,max}/V$.

sive mixer at Re=1 and (c) at Re=50, respectively. Initial condition for the 2-D magnetic mixer is same as Fig. 7. For 3-D passive mixer, 3000 tracers are initially located in the block of $0<x<0.3$, $0.45<y<0.55$ and $0.45<z<0.55$ uniformly, and their projection onto y-z plane is shown in Fig. 16b and 16c. Φ represents the time period in which a tracer located at the center of the channel travels through one unit (different for respective cases). In 2-D magnetic mixer, a number of folding can be already seen after 2.5Φ, and beads are spread all over at $5\sim10\Phi$. In 3-D passive mixer, the flow is totally regular at Re=1, so the initial condition just suffers minor stretching (Fig. 16-b3). At Re=50, some folding patterns are achieved at 5Φ, and tracers spread at 10Φ. However, the number of folding pattern is much less than the active case at the same unit length. Therefore, the 3-D passive mixer requires longer time and length of the mixer to complete the mixing.

CONCLUDING REMARKS

The characteristics of the chaotic micro-mixer of magnetic beads are examined in detail by 2-D numerical simulation. The degree of chaos is quantified by means of the Lyapunov exponent, and the optimum signal frequency is found to exist. Matching of the driving frequency and the flow time constant facilitates chaotic mixing. It is also shown that the probability of attachment of magnetic beads onto bio-molecules is maximized in the chaotic regime.

The difference between our active mixer and the 3-D passive mixer is discussed. Although passive mixers have an advantage in its simplicity, they require the Reynolds number of more than 20 to operate effectively, and relatively longer length is necessary. On the other hand, active mixers can effectively work even in a creeping flow. Thus, the principle of mixing should be appropriately chosen depending on the application.

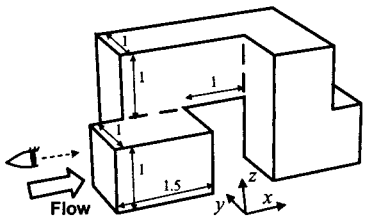

Fig. 14 Three dimensional serpentine passive mixer proposed in Beebe et al (2001).

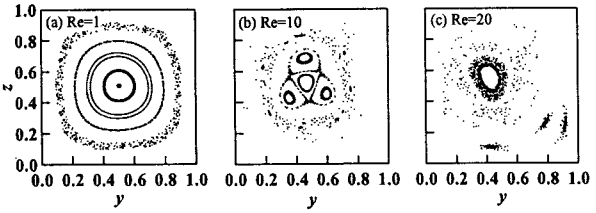

Fig. 15 Poincare sections of 9 tracers at x=0. (a) Re=1, (b) Re=10, and (c) Re=20.

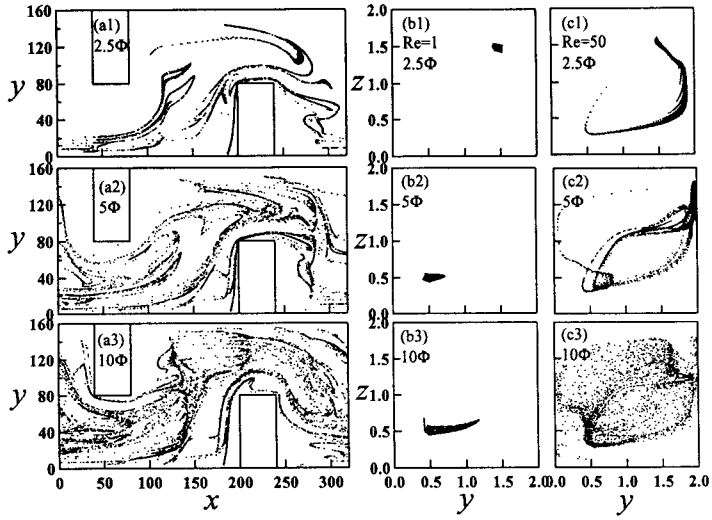

Fig. 16 Particle distribution at different time periods. (a1-a3) 2-D serpentine channel, Re~0.01. (b1-b3) 3-D serpentine channel, Re=1. (c1-c3) 3-D serpentine channel, Re=50.

One of the authors (H. Suzuki) was supported by JSPS Research Fellowship for Young Scientists from 2000 to 2002. The fabrication of the device is mainly funded by DARPA/MTO.

REFERENCES

Beebe, D. J., Adrian, R. J., Olsen, M. G, Stremler, M. A., Aref, H., and Jo., B. H., 2001, "Passive Mixing in Microchannels: Fabrication and Flow Experiments", Mec. Ind., Vol. 2, pp. 343-348.

Burns, M. A., Johnson, B. N., Brahmasandra, S. N., Handique, K., Webster, J. R., Krishnan, M., Sammarco, T. S., Man, P. M., Jones, D., Heldsinger, D., Mastrangelo, C. H., and Burke, D. T., 1998, "An Integrated Nanoliter DNA Analysis Device", Science, Vol. 282, pp. 484-487.

Branebjerg, J., Gravesen, P., Krog, J. P., and Nielsen, C. R., 1996, "Fast Mixing by Lamination", Proc. Ann. Workshop on MEMS, pp. 441-446.

Deval, J., Tabeling, P. and Ho, C. M., 2002, "A Dielectrophoretic Chaotic Mixer", IEEE Proc. Int. Conf. MEMS, pp. 36-39.

Einstein, A., 1905, "On the Movement of Small Particles Suspended in a Stationary Liquid Demanded by the Molecular-Kinetic Theory of Heat", In: Theory of the Brownian Movement, Dover Publications Inc., New York, pp. 1-18.

Lee, Y. K., Deval, J., Tabeling, P. and Ho, C. M., 2001, "Chaotic Mixing in Electrokinetically and Pressure Driven Micro Flows", IEEE Proc. Int. Conf. MEMS, pp. 483-486.

Liu, R. H., Stremler, M. A., Sharp, K. V., Olsen, M. G, Santiago, J. G, Adrian, R. J., Hassan, A., and Beebe, D. J., 2000, "Passive Mixing in a Three-Dimensional Serpentine Microchannel", J. Microelectromechanical Systems, Vol. 9, No. 2, pp. 190-197.

Ho, C. M., 2001, "Fluidics: the Link between Micro and Nano Science and Technologies", IEEE Proc. Int. Conf. MEMS, pp. 375-384.

Manz, A., Graber, N., and Widmer, H. M., 1990, "Miniaturized Total Chemical Analysis Systems: a Novel Concept for Chemical Sensing", Sens. Actuators B1, pp. 221-226.

Möbius, H., Ehrfeld, W., Hessel, V., Richter, Th., 1995, "Sensor Controlled Processes in Chemical Microreactors", Proc. Transducers '95.

Oki, A., Adachi, S., Takamura, Y., Ishihara, K., Ogawa, H., Ito, Y., Ichiki, T., and Horiike, Y., 2001, "Electroosmosis Injection of Blood Serum into Biocompatible Microcapillary Chip Fabricated on Quartz Plate", Electroosmosis, Vol. 22, pp. 341-347.

Ottino, J. M., 1989, "The Kinematics of Mixing: Stretching, Chaos, and Transport", Cambridge University Press.

Ottino, J. M., 1990, "Mixing, Chaotic Advection, and Turbulence", Ann. Rev. Fluid Mech., Vol. 22, pp. 207-253.

Stroock, A. D., Dertinger, S. K. W., Ajdari, A., Mezic, I., Stone, H. A., and Whitesides, G. M., 2002, "Chaotic Mixer for Microchannels", Science, Vol. 295, pp. 647-651

Suzuki, H., and Ho, C. M., 2002, "A Magnetic Force Driven Chaotic Micro-Mixer", IEEE Proc. Int. Conf. MEMS, pp. 40-43

Suzuki, H., 2003, "Development of Chaotic Micro-Mixer Using Magnetic Beads", Doctoral Thesis, Dept. Mech. Eng., The University of Tokyo. http://www.thtlab.t.u-tokyo.ac.jp.

Wolf, A., Swift, J. B., Swinney, H. L., and Vastano, J. A., 1985, "Determining Lyapunov Exponents from a Time Series", Physica 16D, pp. 285-317.